JOURNAL OF ENVIRONMENTAL SCIENCES 57 (2017) 391–401

Available online at www.sciencedirect.com

ScienceDirect

www.elsevier.com/locate/jes

JES JOURNAL OF ENVIRONMENTAL SCIENCES

www.jesc.ac.cn

Numerical simulation of flow hydrodynamics of struvite pellets in a liquid–solid fluidized bed

Xin Ye[1], *Dongyuan Chu*[1,2], *Yaoyin Lou*[1], *Zhi-Long Ye*[1], *Ming Kuang Wang*[3], *Shaohua Chen*[1,*]

1. *Key Laboratory of Urban Pollutant Conversion, Institute of Urban Environment, Chinese Academy of Sciences, Xiamen 361021, China*
2. *College of the Environment and Ecology, Xiamen University, Xiamen 361102, China*
3. *Fujian Academic of Agricultural Sciences, Fuzhou 350003, China*

ARTICLE INFO

Article history:
Received 4 August 2016
Revised 23 September 2016
Accepted 7 November 2016
Available online 30 December 2016

Keywords:
Numerical simulation
Flow hydrodynamics
Struvite
Liquid–solid fluidized bed

ABSTRACT

Phosphorus recovery in the form of struvite has been aroused in recent decades for its dual advantages in eutrophication control and resource protection. The usage of the struvite products is normally determined by the size which is largely depended on the hydrodynamics. In this study, flow behavior of struvite pellets was simulated by means of Eulerian–Eulerian two-fluid model combining with kinetic theory of granular flow in a liquid–solid fluidized bed reactor (FBR). A parametric study including the mesh size, time step, discretization strategy, turbulent model and drag model was first developed, followed by the evaluations of crucial operational conditions, particle characteristics and reactor shapes. The results showed that a cold model with the mesh resolution of 16 × 240, default time step of 0.001 sec and first order discretization scheme was accurate enough to describe the fluidization. The struvite holdup profile using Syamlal–O'Brien drag model was best fitted to the experimental data as compared with other drag models and the empirical Richardson–Zaki equation. Regarding the model evaluation, it showed that liquid velocity and particle size played important roles on both solid holdups and velocities. The reactor diameter only influenced the solid velocity while the static bed height almost took no effect. These results are direct and can be applied to guide the operation and process control of the struvite fluidization. Moreover, the model parameters can also be used as the basic settings in further crystallization simulations.

Introduction

Phosphorus removal and recovery from waste streams or solids has been considered as the spotlight in both eutrophication control and resource protection aspects in recent decades (Desmidt et al., 2015; Schoumans et al., 2015). One of the prevalent techniques, namely struvite ($MgNH_4PO_4{\cdot}6H_2O$) crystallization, has been widely adopted, which can simultaneously recover phosphorus and nitrogen in the form of struvite in the presence of magnesium ions at weak alkaline conditions (Le Corre et al., 2009). The harvested struvite can be used as a slow-release fertilizer or rehabilitating agent of the oligotrophic streams depending on the sizes (Sterling and Ashley, 2003). Up to date in the struvite crystallization system, a number of chemical equilibrium models and kinetics models were successfully developed to aid the reactor design and operation (Ali and Schneider, 2008; Galbraith et al., 2014). It showed that larger crystals can be harvested once the

* *Corresponding author*.
E-mail addresses: xye@iue.ac.cn (X. Ye), shchen@iue.ac.cn (S. Chen).

http://dx.doi.org/10.1016/j.jes.2016.11.019

supersaturation was maintained in the metastable zone (Ali and Schneider, 2005). However, as can be seen from image evidences (Fattah et al., 2012; Forrest et al., 2008), secondary effects deriving from hydrodynamics, such as aggregation and breakage seemed more crucial to the size enlargement (Vedantam and Ranade, 2013). It has been reported in struvite crystallization that crystallizer type (fluidization, agitation or jet-pump) and hydraulic intensity (upflow liquid velocity or stirring speed) would influence the crystal size distribution (Le Corre et al., 2009), implying the importance of the hydrodynamics, but the knowledge of hydrodynamics has not been systematically investigated. In addition to gain larger size products, efficient design of a crystallization reactor is considered reliable heavily upon the knowledge of reactor hydrodynamics besides thermodynamics and process kinetics (Rahaman et al., 2014b).

Hydrodynamics plays a key role in mixing and fluidization in the struvite FBR, the description of flow behavior is challenging due to complex solid–liquid interactions. Generally, solid holdup and solid velocity are used to represent the flow behavior, which can be measured by several methods, such as optical fiber probe (Miao et al., 2011), particle image velocimetry (PIV) (Reddy et al., 2013) or computer-aided radioactive particle tracking (CARPT) (Limtrakul et al., 2005). Experimental measurements can provide accurate and reliable data but would have some restrictions. Moreover, these instruments are normally expensive, complex to operate and somewhat dangerous. In addition to experimental investigation, numerical simulation can be a promising alternative. Computational fluid dynamics (CFD) simulation would give detailed information about the local solid holdups and their spatial distributions, flow patterns, and the interaction with other phases (Wang et al., 2010). Such information can be useful in the understanding of the transport phenomena in FBR, and thereafter for the reactor design, operation and optimization (Cornelissen et al., 2007). Although a number of numerical simulations and experimental observations have been done in the liquid–solid FBR, the hydrodynamics investigation of the struvite fluidization is far from needed (Rahaman and Mavinic, 2009; Rahaman et al., 2014a). Because different flow behavior of the struvite pellets would be expected for their ellipsoidal type with numerous pores and defects (Fattah et al., 2012), unlike with the spherical and solid materials previously used in the literatures (Cornelissen et al., 2007; Wang et al., 2010), a systematic study with regard to the struvite hydrodynamics is urgently required.

In CFD simulations, two different types of models are usually used to describe the flow characteristics in the liquid–solid FBR. One is the Eulerian–Lagrangian (E–L) approach and the other is Eulerian–Eulerian (E–E) two-fluid model. In the E–L approach, the carrier phase is considered as a continuous phase and the solid phase is treated as a discrete phase and solved by tracking a large number of particles. While in the E–E approach, the different phases are treated mathematically as interpenetrating continua. The E–E approach is more attractive in simulating FBR for it has no limitations on the particle volume fraction and needs less computational resource. In order to integrate useful solid information, such as shear stress, bulk viscosities and fluctuating energies, the equations in the granular E–E model are closed by the application of kinetic theory of granular flows (KTGP). Another important closure problem arises due to the interphase momentum transfer, which can be well described by various drag laws (Gidaspow et al., 1992; Lu and Gidaspow, 2003; Syamlal and O'Brien, 1989; Wen and Yu, 1966). The inappropriate use of drag laws outside their applicable scopes would lead to unsatisfactory results. Therefore, before a numerical model can be used, a systematic parametric estimation including the optimization of drag laws should be first carried out.

In this study, besides exploring the hydrodynamic characteristics experimentally, CFD is used to predict the flow patterns, solids holdups and velocities of the struvite pellets in a FBR. Firstly, several model input or solution parameters—mesh resolution, time step, discretization scheme, turbulent model and drag model—are optimized to establish a suitable model for the struvite fluidization system. After model validation by the experimental data, the influences of operational conditions (initial static bed height and liquid velocity), particle size and reactor diameter are investigated subsequently.

1. CFD modeling

1.1. Computational geometry

A column FBR was set up for both experimental and numerical investigations. The experimental reactor was built of plexiglas and had a diameter of 80 mm and a height of 1200 mm (Fig. 1a). A distributor, consisted of 0.15 mm sieve, 3 mm-orifices plate and 4 mm-glass beads, was installed below the column to homogenize the inflow. The fluidized materials were the struvite pellets and the characteristic, such as size and density, were determined previously (Table 1). The deionized water saturated with struvite was used to avoid the dissolution. The averaged solid holdup was measured accordingly for the verification and optimization of the cold model (Cornelissen et al., 2007). Pressure ports along the wall were connected to pressure transducers (HM22, Germany) and the voidages were estimated from the pressure drop measurements, and then converted to the solid holdup (Dhanuka and Stepanek, 1978).

1.2. Model formulation

A 2D two-fluid model based on the E–E approach was employed to describe the fluidization behavior of struvite in the column. The model considered the conservation of mass and momentum for the solid and liquid phases, and incorporates KTGF for closure of solids stress terms. Only the drag force was included for interphase momentum transfer due to its significance (Cornelissen et al., 2007). The turbulent behavior was described by turbulent models. Altogether, four empirical drag laws and three turbulent models were compared for better accuracy. All the governing equations are extensively presented in literatures (Cornelissen et al., 2007; Yan et al., 2011) and thus only summarized in Supplementary data (Table S1) for concise purpose.

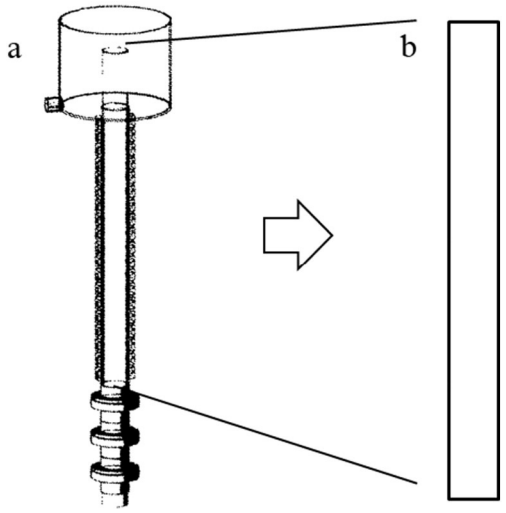

Fig. 1 – Geometry of the fluidized bed reactor. (a) Real geometry; (b) 2D geometry of the full fluidization zone.

1.3. Numerical methodology

The fluidization zone of the FBR was simplified to a two-dimensional (2D) rectangle (Fig. 1b), which was meshed using Gambit 2.4.6, and then exported into FLUENT 14.5 for calculation in a double precision mode. The phase coupled SIMPLE algorithm was employed for the pressure–velocity coupling. Velocity inlet, pressure outlet and no-slip wall were used as the boundary conditions. The convergence criterion was set at 1×10^{-4} for all the equations. All the simulations were performed in a platform of Intel 2.83 GHz Xeon with 64 GB of RAM.

Before the case evaluation, comprehensive model parameter investigations and verifications were carried out. The optimization included the comparisons of mesh resolutions, time steps, discretization strategies, turbulent models and drag models. Once the fully developed quasi-steady state was reached, time-averaged solid holdups were used to assess the accuracy of the model. The base case settings and parametric studies were illustrated in Table 2. Mesh, time step, discretization and turbulent model were first investigated by comparing with the experimental results using the moderate level of pellets size (*e.g.*, 1.6–2.0 mm) and superficial velocity (*e.g.*, 0.05 m/sec). Afterwards, drag models were further evaluated using various liquid velocities and pellet sizes. An empirical correlation, namely Richardson–Zaki equation (Richardson and Zaki, 1954), was also presented for comparison in the present work. Once the parameter investigations and verifications were finished, case evaluations were carried out by varying the initial static bed height, liquid velocity, particle size and reactor diameter.

Table 1 – Characteristics of the struvite pellets.

Sieved size range (mm)	Volume equivalent diameter (mm)	Density (kg/m)	Minimum fluidization velocity (mm/sec)
0.9–1.25	1.06	1579	0.005
1.6–2.0	2.21	1580	0.015
2.8–3.2	3.37	1588	0.023
4.0–5.0	4.45	1587	0.032

2. Results and discussion

2.1. Model optimization and verification

Key model parameters were compared according to the settings as shown in Table 2. All of the comparisons were done after the bed had been fully expanded.

2.1.1. Mesh, time step, discretization and turbulent model optimizations

The mesh independence was examined using five different grids, 11 × 60, 11 × 120, 16 × 240, 32 × 480 and 64 × 960. It indicates that model with the moderate mesh resolution best fits the experimental data, either coarse or fine grids would result in underestimated expansion behaviors (Fig. 2a). The result from 16 × 240 grid deviates less than 2% from the experimental data and consumes less time as compared with the one using finer mesh (*i.e.*, 32 × 480) and is thus used in the

Table 2 – Base case settings and parametric studies.

Mesh	Time step (sec)	Discretization scheme	Turbulent model	Drag model
11 × 60	0.0005	**First order upwind + VOF_{first}**	**Mixture**	Syamlal–O'Brien
11 × 120	**0.001**	second order upwind + VOF_{first}	Dispersed	Wen and Yu
16 × 240	0.005	first order upwind + VOF_{HRIC}	Per phase	**Gidaspow**
32 × 480	0.01	first order upwind + VOF_{QUICK}		Huilin–Gidaspow
64 × 960	0.02			

Bold values are base case settings.

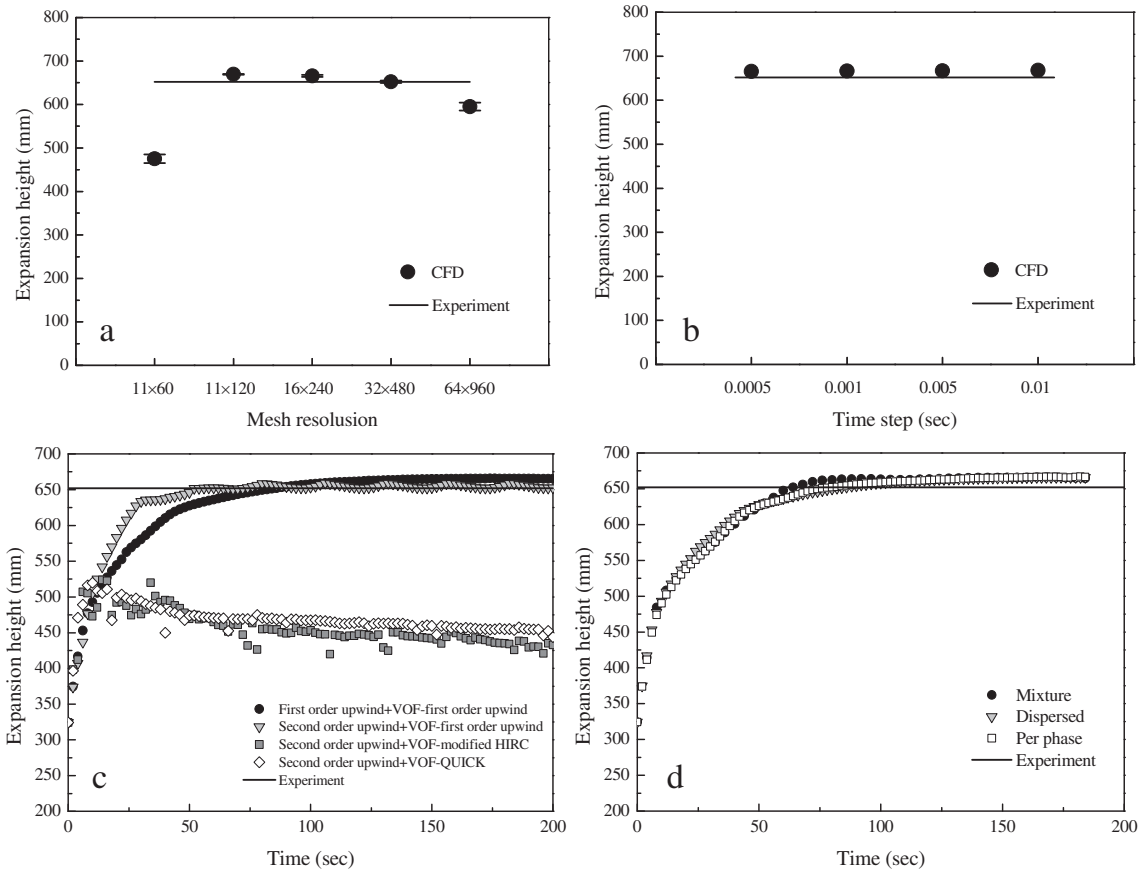

Fig. 2 – Model optimization and verification. (a) Mesh resolution; (b) time step; (c) discretization scheme; (d) turbulent model. CFD: computational fluid dynamics; VOF: volume fraction.

following studies. Regarding time steps, fixed steps ranging from 0.0005 to 0.01 sec provide very similar results close to the experimental value (Fig. 2b), while the step of 0.02 sec encounters a difficulty in convergence (data not shown). A time step of 0.001 sec has often been used for meeting the accurate and stable requirement in literatures and thus chosen in this study (Cornelissen et al., 2007). For the comparison of discretization schemes, first and second order upwind differencing schemes can well fit the experimental data, whereas higher discretization schemes of volume fraction (VOF), such as modified version of the High Resolution Interface Capturing (HRIC) scheme and Quadratic Upwind Interpolation of Convective Kinematics (QUICK) scheme give unphysical results (Fig. 2c). Although second order upwind differencing scheme shows better performance than first order upwind scheme, it is much more computationally expensive. Therefore, first order upwind scheme is used in the following calculations. It can be seen that the predictions using different turbulent models are in good agreements with the experimental data, which indicates the minor effect of turbulence in the struvite fluidization system (Fig. 2d). Same turbulent results are obtained in the liquid–solid circulating fluidized bed system (Zheng and Zhu, 2003). However, it should be noted that the mixture k-ε model may become unsuitable when the density ratio between the two phases is much higher than 1 (Dadashi et al., 2014). Because the density of struvite is at least 50% higher than the liquid phase, the dispersed turbulent model is thus used for accuracy.

2.1.2. Drag model optimization

In literatures, several drag models are widely used to describe the liquid–solid interaction, such as Syamlal–O'Brien (Syamlal and O'Brien, 1989), Wen and Yu (Wen and Yu, 1966), Gidaspow (Gidaspow et al., 1992) and Huilin–Gidaspow (Lu and Gidaspow, 2003). Each model has its own scope of application. For example, the Wen and Yu model is appropriate for dilute systems while the Gidaspow model is recommended for dense fluidized beds. In the struvite fluidization system, the "dilute" or "dense" stage is difficult to distinguish due to the multi-class of the struvite pellet sizes. In such a situation, smaller size pellets are tended to expand to the higher region while larger ones would accumulate at the bottom, implying that both "dilute" and "dense" conditions exist in one fluidization system. Therefore, it is essential to evaluate the accuracy of drag models for the struvite fluidization system. The process conditions used for this simulation are liquid superficial velocity of 0.033, 0.050 and 0.066 m/sec, which denote 2.2, 3.3 and 4.4 times of the minimum fluidization velocity (u_{mf}) of the 1.6–2.0 mm struvite pellets. The solid holdup profiles obtained by CFD simulation along with the experimental result and Richardson–Zaki equations are summarized in Table 3. The deviations (Dev) of the simulated

Table 3 – Solid holdup comparisons using different drag laws.*

v_l	Solid holdups					
(m/sec)	Exp.	Gidaspow	Wen and Yu	Huilin–Gidaspow	Syamlal–O'Brien	Richardson–Zaki
0.033	0.441	0.401	0.423	0.399	0.405	0.432
0.050	0.300	0.265	0.339	0.268	0.295	0.334
0.066	0.202	0.203	0.271	0.204	0.203	0.254
Dev.*		9.36×10^{-4}	2.20×10^{-3}	9.11×10^{-4}	4.41×10^{-4}	1.31×10^{-3}

* Deviation calculated using Eq. (1).

results and empirical equations from the experimental results are compared (Eq. (1)), where lower deviation value implies better accuracy.

$$\text{Dev} = \frac{\sum_{i=1}^{N}\left(\varepsilon_{sim_i} - \varepsilon_{exp_i}\right)^2}{N} \quad (1)$$

where, ε represents the solid holdup, and the subscripts of "sim_i" and "exp_i" denote the simulated and experimental results, respectively.

It can be observed that the deviation values for the CFD simulations range from 4.41×10^{-4} to 2.20×10^{-3}, lower than that calculated by empirical equations. Among the drag models, results based on the Syamlal–O'Brien and Huilin–Gidaspow are closer to the experimental results than that of results obtained by other drag models.

By considering the coexistence of multiple size pellets in the struvite fluidization system, two best drag models, *i.e.*, Huilin–Gidaspow and Syamlal–O'Brien, were further compared in four size ranges. As can be seen from Table 4, Syamlal–O'Brien drag model again shows the best predictive accuracy with the total deviation value of 5.55×10^{-3}, only half as compared with ones in Huilin–Gidaspow drag model and Richardson–Zaki equation. Therefore, Syamlal–O'Brien is the most appropriate drag model in the struvite fluidization system.

In summary, the parameters suitable for the struvite fluidization system are as follows: mesh resolution of 16 × 240, time step of 0.001 sec, dispersed turbulent model, first order upwind discretization strategy and Syamlal–O'Brien drag model. Such settings are kept constant in the subsequent model identifications.

2.2. Model identification

2.2.1. Features of simulated struvite fluidization system

To explore the characteristic of struvite fluidized beds, the solid holdups as well as the solid velocities were investigated. Fig. 3a shows instantaneous snapshots of the struvite holdup distributions in the fluidized bed. It shows that the solid bed expands within the first period of time. The flow structure seems asymmetrical where a solid voidage wave appears in the core. When the quasi-steady state is reached, the solid holdup profile is found to be relatively uniform across the column. The instantaneous velocity vector distribution in Fig. 3b clearly shows a core–annular flow structure. The profile of the structure remains stable once the solid bed is fully expanded, although the velocity slightly sways in the upper region.

Table 4 – Deviation comparisons using different drag laws.

Sieved size (mm)	Dev. value		
	Huilin–Gidaspow	Syamlal–O'Brien	Richardson–Zaki
0.9–1.25	1.94×10^{-3}	1.79×10^{-3}	1.21×10^{-3}
1.6–2.0	9.11×10^{-4}	4.41×10^{-4}	1.31×10^{-3}
2.8–3.2	3.81×10^{-3}	2.28×10^{-3}	1.60×10^{-3}
4.0–5.0	2.90×10^{-3}	1.03×10^{-3}	5.75×10^{-3}
Total Dev.	9.56×10^{-3}	5.55×10^{-3}	9.87×10^{-3}

As reported in the liquid–solid fluidized bed, the dynamic solid flow structure consists two pairs of counter-rotating recirculation cells, which is, up at the outside and down in the middle near the distributor and reverse in the upper region of the bed (Limtrakul et al., 2005). However in this study, only one single circulation pattern can be observed, where solids move upward in the core and downward near the wall across the bed. The difference is possibly because of the diverse densities of fluidized materials. Glass beads with density of 2500–3000 kg/m^3 were largely used in literatures, while the density of struvite pellets tested in this study were only 1500 kg/m^3. As can be seen from Fig. 4a, the solid velocity near the distributor fluctuates probably due to the turbulence created by the random motions of the liquid phase (Wang et al., 2010). Afterwards, the solid axial velocity is enhanced drastically above the inlet area and lowed at the upper region. Moreover, the solids show various radial velocity profiles. As the position moves from the core to the wall, the solid velocity is lowered and then reversed (Fig. 4a). In such a case, the transition point at dimensionless radius is between 0.5 and 0.6, as compared to the glass beads where the value of 0.6–0.7 was found (Limtrakul et al., 2005). The recirculation of struvite pellets can also be verified by the axial solid velocity at different radial positions. From Fig. 4b, the axial solid velocity shows a descending trend from the core to the transit point, and then, reverses and increases until the wall. This phenomenon is obvious at the lower part of the column where more energy is derived from the inflow. Afterwards, the differences become small as the height increases. To better explore the effect of parameters, *i.e.*, static bed height, liquid velocity, particle size and reactor diameter, the radial solid holdups and velocities at height of 0.1 and 0.3 m, as well as axial ones at the core of the column (x/R = 0), are compared in subsequent studies.

2.2.2. Influence of static bed height

The static bed height is important in the struvite fluidization system for it reflects the solid amounts at the static stage. Fig. 5 shows the profiles of solid holdup and axial velocity at three

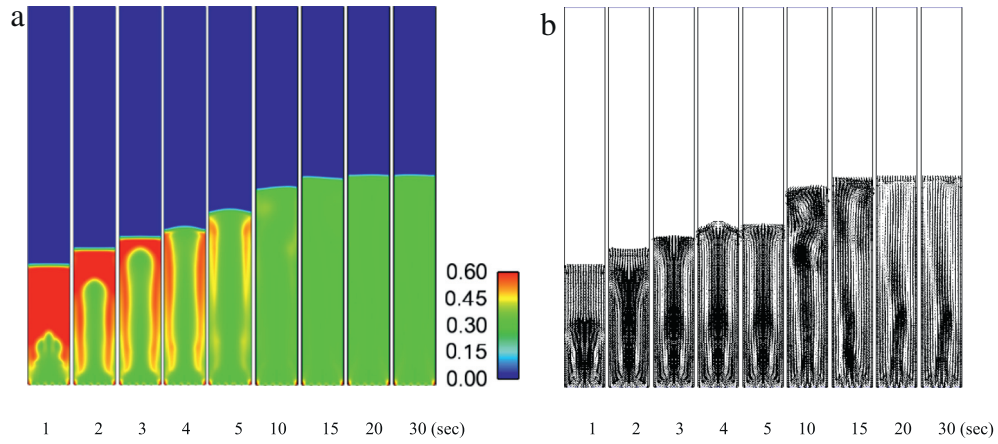

Fig. 3 – Instantaneous distribution at superficial liquid velocity of 0.05 m/sec. (a) Struvite holdup; (b) struvite velocity vector.

static bed heights. Once the quasi-steady state is reached, the solid holdup profile is found to be relatively uniform across the column. Although larger static bed height shows higher expansion height, the same solid holdup with the value of 0.27 is found regardless of the initial differences (Fig. 5a). Same profile of axial solid velocity can also be seen along the fluidized bed. It indicated that particles are speeded up at the lower axial position, where same particle velocity up to 0.10 m/sec can be reached in all the three cases. Afterwards, the core velocity is lowered gradually along the solid beds (Fig. 5a).

Almost same radial distributions of solid holdup can be seen at the same axial positions (Fig. 5b). The holdup of struvite pellets is slightly higher near the walls and lower in the center of the bed, while this distribution becomes uniform at the higher region. The profile of the solid velocities displayed a contrary trend as compared with the holdups, where the highest value appears in the core area (Fig. 5b). This phenomenon is mainly dependent on the velocity distribution of the fluidized liquid, which is static at wall but more active in the middle of a pipe or two plates due to its intrinsic viscosity (Xia and Chen, 2007). Therefore, a parabolic or parabolic-like distribution of liquid velocity is commonly found along the flow direction and subsequently affects the velocities of the particles.

As mentioned above, it indicates that the static bed height has very little influence on the solid holdup and the velocity either axially or radially. This conclusion can also be supported by other fluidization system either experimentally or numerically (Limtrakul et al., 2005; Wang et al., 2010). Moreover, the inessential effect of the static bed height can also be inferred from the u_{mf} measurement, where the static bed heights were set randomly but same results of pressure drop (or solid holdup) can be obtained (Ma et al., 2012; Li et al., 2013).

2.2.3. *Influence of liquid velocity*

Fig. 6 shows the axial and radial profiles of the 1.6–2.0 mm struvite pellets at three liquid velocities. Different from the static bed height, the effect of the liquid velocity is obvious, which influences the holdups and velocities both axially and radially. As shown in Fig. 6a, the struvite axial velocity increases with the increase of liquid velocity, and brings about two apparent phenomena, namely (1) the increase of the maximal velocity value of the pellets and (2) the increase of the expansion height. The explanation is that higher liquid velocity denotes larger energy input, leading to the increase in turbulence and then the

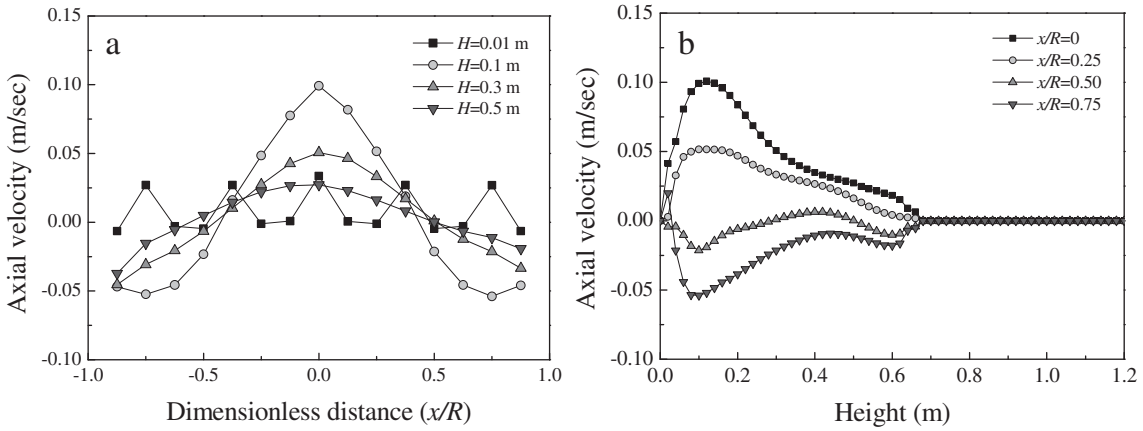

Fig. 4 – Distribution of the time-average struvite velocity along the (a) radial and (b) axial direction. *H*: axial height; *x/R*: dimensionless distance.

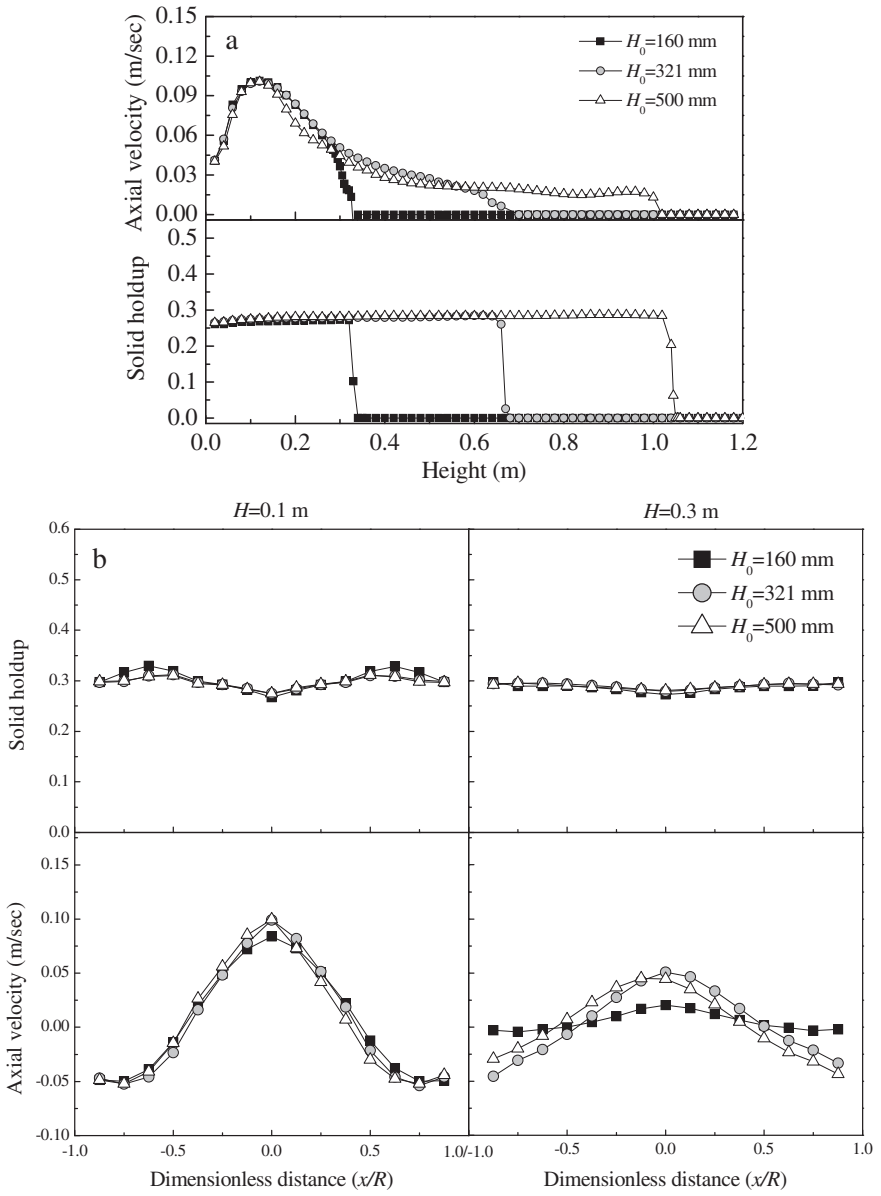

Fig. 5 – Distribution of struvite holdups and velocities at different static bed heights (H_0). (a) Holdups and axial velocities along the axial direction; (b) holdups and axial velocities along the radial direction.

solids circulation (Limtrakul et al., 2005). Moreover, higher liquid velocity normally corresponds to lower solid holdup. Although the liquid velocity is increased, the solid bed is expanded uniformly across the column. Therefore, the liquid velocity can be used as a direct method to regulate the struvite holdup in the fluidized bed reactor, to satisfy the fluidization and fines control purpose, simultaneously (Ye et al., 2016).

Different radial distributions of solid holdup can be seen at the same axial positions (Fig. 6b). Corresponding to the axial profile of solid holdups, a higher liquid velocity gives a lower holdup of the struvite pellets. The holdups in all the three cases are slightly higher near the wall and lower in the center of the bed regardless of the variety of the liquid velocity. The profile of the solid velocities displayed a contrary trend as compared with the holdups, where the highest value appears in the core area. The difference of the solid velocities is not obvious near the inlet area (H = 0.1 m), but higher liquid velocity denotes larger velocity as the height increases (H = 0.3 m). It should be noted that the solid velocity is actually lowered when the particles are fluidized into the upper region, where the inlet energy takes reducing impact as compared with the inlet area. It can also be observed that the solid velocity inversion point (opposite velocity directions on its both sides) shifts from 0.42 to 0.63 when the liquid velocity is doubled (*e.g.*, from 0.033 to 0.066 m/sec).

From the foregoing discussion, it can be concluded that the liquid velocity plays an important role in the distribution behavior of the struvite pellets.

2.2.4. *Influence of particle size*

Fig. 7 shows the profiles of solid holdup and axial velocity at three struvite sizes. Previously in the experimental study,

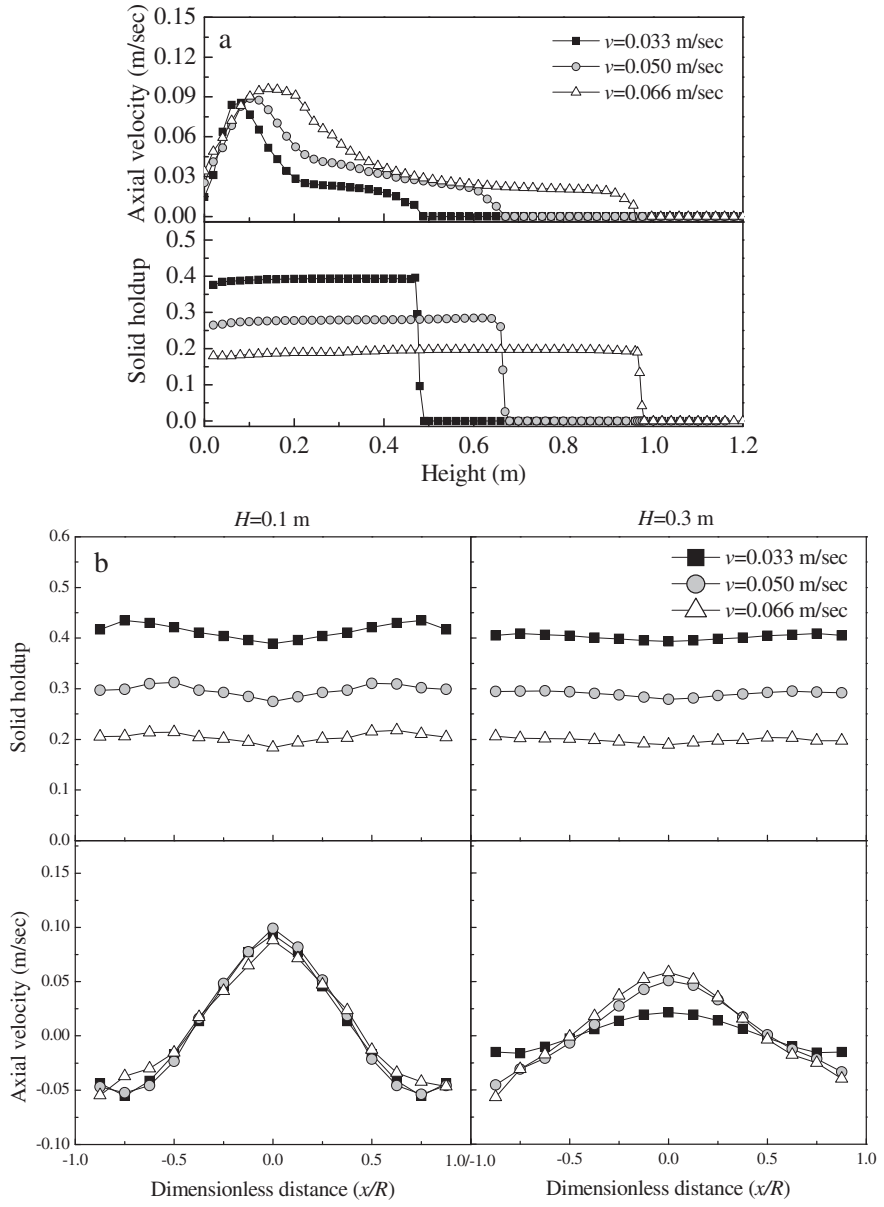

Fig. 6 – Distribution of struvite holdups and velocities at different liquid velocities (*v*). (a) Holdups and axial velocities along the axial direction; (b) holdups and axial velocities along the radial direction.

struvite pellets with larger size possessed lower expansion index, which indicates a higher solid holdup at the same liquid velocity (Rahaman et al., 2014a). The reported results can also be reappeared in the simulation, where the solid holdup shows the same relationship with the liquid velocity (Fig. 7a). In fluidization systems with multi-class sizes, larger particles tend to reach the bottom of the reactor, whereas smaller particles rises (Rahaman and Mavinic, 2009). Therefore, a classification phenomenon might be happening once the liquid velocity is inadequate (Reddy and Joshi, 2009). Corresponding to the holdup profile, the solid velocity shows a contrary trend. Although same energy is input through the upflow liquid, particles with smaller sizes would gain a higher velocity as compared with the larger ones. This implies that more frequent collisions happen among small particles, and thereafter, a larger and more compact pellet would form *via* the aggregation mechanism (Ye et al., 2014). Besides considering the differences under a unique liquid velocity, the axial solids holdups and velocities are also evaluated at a given v_l/u_{mf} (Fig. 7b). In these cases, a multiple of 2.2 is used, which is equal to the liquid velocities of 0.034, 0.050 and 0.072 m/sec for sizes of 1.6–2.0, 2.8–3.2 and 4.0–5.0 mm, respectively. With the increase of particle size, the profiles of axial solids velocities and holdups at given v_l/u_{mf} exhibit contrary trends as compared under single liquid velocity discussed previously (Fig. 7a). Similar phenomenon can be found in a liquid–solid fluidized bed using glass and acetate beads as the fluidization materials (Limtrakul et al., 2005). Since the particle sizes in this study do not differ too much, the impact is not as obvious as the liquid velocity, which leads to some overlapping of the axial profiles, especially at the height investigated (*i.e.*, H = 0.1 and 0.3 m). Therefore, the radial profiles of solid holdups and

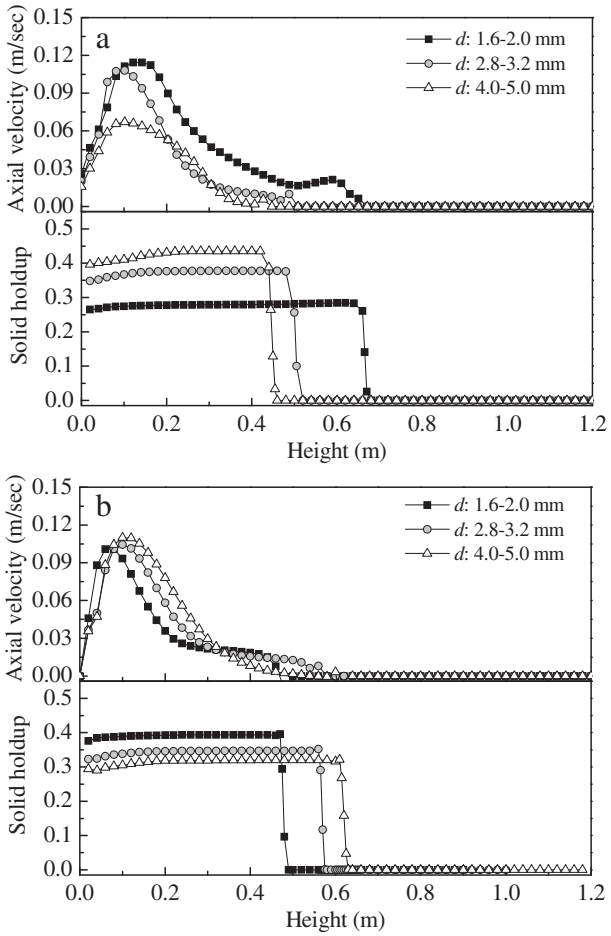

Fig. 7 – Distribution of struvite holdups and velocities at different particle sizes (*d*). (a) Under the same liquid velocity; (b) under the same ratio of liquid velocity to minimum fluidization velocity, v_l/u_{mf} = 2.2.

velocities are not shown in this section. However, the movement of the velocity inversion points to the center also can be observed at some distinguishing position (*e.g.*, *H* = 0.2 m) as the size increases (data not shown), similar to the investigations in the bubble column or liquid–solid fluidized bed (Limtrakul et al., 2005; Rice and Geary, 1990).

2.2.5. Influence of reactor diameter

To retain fine crystals in the FBR, one of the effective methods is to lower the crystal velocities by increasing the reactor diameter (Fattah et al., 2012). Moreover, different diameters would result in solid classification under the same liquid velocity. Fig. 8 shows the profiles of solid holdup and axial velocity at three reactor diameters. At a given liquid velocity (*e.g.*, 0.050 m/sec), the maximal value of axial solid velocity in the 160 mm-reactor is almost 2.62 times of that in the 40 mm-reactor (Fig. 8a), which is mainly due to the larger eddies in the bigger reactor and comparable with the previous study (Limtrakul et al., 2005). Higher solid velocity would lead to stronger collisions, resulting in breakage of the particles, while mild velocities would hamper the compactness of the solids (Fattah et al., 2012). Therefore, for the sake of appropriate hydrodynamics, the choice of the reactor diameter is important and should be paid more attention. Regarding the solid holdup either axially or radially, almost same profile can be found regardless of the reactor diameters (Fig. 8a,b). However, the solid velocity differs strongly along the radial direction as can be seen in Fig. 8b, that is, higher solid velocity in the center derives from the larger reactor diameter due to more energy input. Although big differences exist, no significant shift of velocity inversion points can be observed.

It can be concluded that the reactor diameter mainly influences the solid velocity while takes no effect on the distribution of solid holdups.

3. Conclusions

A CFD model based on the kinetic theory of granular flow has been successfully applied to investigate the flow behavior of struvite pellets in a fluidized bed reactor. The crucial modeling parameters were first estimated and the optimized results are shown as follows: mesh resolution of 16 × 240, time step of 0.001 sec, dispersed turbulent model, first order upwind discretization strategy and Syamlal–O'Brien drag model. With these settings, the predicted values were in good agreement with the experimental values, even better

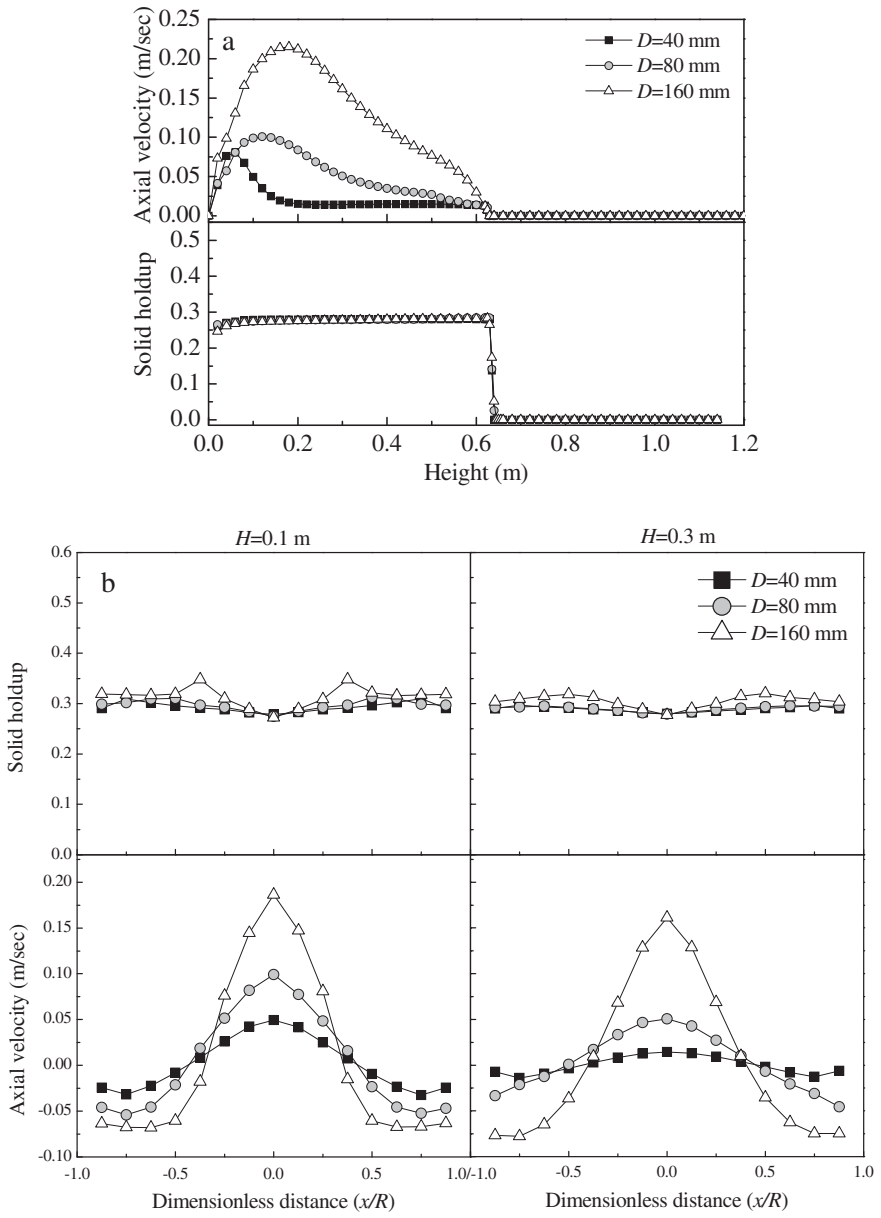

Fig. 8 – Distribution of struvite holdups and velocities at different reactor diameters (*D*). (a) Holdups and axial velocities along the axial direction; (b) holdups and axial velocities along the radial direction.

than the ones calculated from the empirical Richardson–Zaki equation. The model was evaluated through changing the operational conditions, particle characteristics and reactor shapes. It showed that the liquid velocity and particle size played important roles on both the solid holdups and velocities. The reactor diameter only influenced the solid velocity while the static bed height took no effect. Having known these effects, one can intensify the struvite granulation by increasing either liquid velocity or reactor diameter and make a harvesting plan by controlling the static bed height to avoid any entrainment of the target products. The results are direct and can be applied to guide the operation and process control of the struvite fluidization. Moreover, the parameters optimized in the cold model can be also used as the basic settings in further struvite crystallization simulations, in which cases, more complex thermodynamics and kinetics will be included besides hydrodynamics.

Acknowledgments

The work was supported by the Young Scientists Frontier Foundation of Institute of Urban Environment, Chinese Academy of Sciences (No. IUEQN201501) and the National Natural Science Foundation of China (No. 51608503). Additionally, the authors are grateful to Jingcai Cheng from the Institute of Process Engineering, Chinese Academy of Sciences, for his kindly help in CFD modeling.

Appendix A. Supplementary data

Supplementary data to this article can be found online at http://dx.doi.org/10.1016/j.jes.2016.11.019.

REFERENCES

Ali, M.I., Schneider, P.A., 2005. Crystallization of struvite from metastable region with different types of seed crystal. J. Non-Equilib. Thermodyn. 30 (2), 95–111.

Ali, M.I., Schneider, P.A., 2008. An approach of estimating struvite growth kinetic incorporating thermodynamic and solution chemistry, kinetic and process description. Chem. Eng. Sci. 63 (13), 3514–3525.

Cornelissen, J.T., Taghipour, F., Escudié, R., Ellis, N., Grace, J.R., 2007. CFD modelling of a liquid–solid fluidized bed. Chem. Eng. Sci. 62 (22), 6334–6348.

Dadashi, A., Zhu, J., Zhang, C., 2014. A computational fluid dynamics study on the flow field in a liquid–solid circulating fluidized bed riser. Powder Technol. 260 (7), 52–58.

Desmidt, E., Ghyselbrecht, K., Zhang, Y., Pinoy, L., Van der Bruggen, B., Verstraete, W., et al., 2015. Global phosphorus scarcity and full-scale P-recovery techniques: a review. Crit. Rev. Environ. Sci. Technol. 45 (4), 336–384.

Dhanuka, V., Stepanek, J., 1978. Gas and Liquid Hold-up and Pressure Drop Measurements in a Three-phase Fluidized Bed. Cambridge University Press, Cambridge, UK.

Fattah, K.P., Mavinic, D.S., Koch, F.A., 2012. Influence of process parameters on the characteristics of struvite pellets. J. Environ. Eng. 138 (12), 1200–1209.

Forrest, A., Fattah, K.P., Mavinic, D.S., Koch, F., 2008. Optimizing struvite production for phosphate recovery in WWTP. J. Environ. Eng. 134 (5), 395–402.

Galbraith, S., Schneider, P., Flood, A., 2014. Model-driven experimental evaluation of struvite nucleation, growth and aggregation kinetics. Water Res. 56 (56C), 122–132.

Gidaspow, D., Bezburuah, R., Ding, J., 1992. Hydrodynamics of circulating fluidized beds: kinetic theory approach. Fluidization VII, Proceedings of the Seventh Engineering Foundation Conference on Fluidization. New York, pp. 75–82.

Le Corre, K., Valsami-Jones, E., Hobbs, P., Parsons, S., 2009. Phosphorus recovery from wastewater by struvite crystallization: a review. Crit. Rev. Environ. Sci. Technol. 39 (6), 433–477.

Li, J.G., Cheng, Z.H., Fang, Y.T., Wang, H.Y., Nie, W., Huang, J.J., et al., 2013. Minimum and terminal velocity in fluidization of coal gasification materials and coal blending of gasification under pressure. Fuel 110 (10), 153–161.

Limtrakul, S., Chen, J.W., Ramachandran, P.A., Dudukovic, M.P., 2005. Solids motion and holdup profiles in liquid fluidized beds. Chem. Eng. Sci. 60 (7), 1889–1900.

Lu, H.L., Gidaspow, D., 2003. Hydrodynamics of binary fluidization in a riser: CFD simulation using two granular temperatures. Chem. Eng. Sci. 58 (16), 3777–3792.

Ma, J., Chen, X., Liu, D., 2012. Minimum fluidization velocity of particles with wide size distribution at high temperatures. Powder Technol. 235 (2), 271–278.

Miao, Q., Wang, C., Wu, C., Yin, X., Zhu, J., 2011. Fluidization of sawdust in a cold model circulating fluidized bed: experimental study. Chem. Eng. J. 167 (1), 335–341.

Rahaman, M.S., Mavinic, D.S., 2009. Recovering nutrients from wastewater treatment plants through struvite crystallization: CFD modelling of the hydrodynamics of UBC MAP fluidized-bed crystallizer. Water Sci. Technol. 59 (10), 1887–1892.

Rahaman, M.S., Mavinic, D.S., Ellis, N., 2014a. Fluidisation behaviour of struvite recovered from wastewater. J. Environ. Eng. Sci. 9 (2), 137–149.

Rahaman, M.S., Mavinic, D.S., Meikleham, A., Ellis, N., 2014b. Modeling phosphorus removal and recovery from anaerobic digester supernatant through struvite crystallization in a fluidized bed reactor. Water Res. 51 (51), 1–10.

Reddy, R.K., Joshi, J.B., 2009. CFD modeling of solid–liquid fluidized beds of mono and binary particle mixtures. Chem. Eng. Sci. 64 (16), 3641–3658.

Reddy, R.K., Sathe, M.J., Joshi, J.B., Nandakumar, K., Evans, G.M., 2013. Recent developments in experimental (PIV) and numerical (DNS) investigation of solid–liquid fluidized beds. Chem. Eng. Sci. 92 (1), 1–12.

Rice, R.G., Geary, N.W., 1990. Prediction of liquid circulation in viscous bubble columns. AIChE J. 36 (9), 1339–1348.

Richardson, J.F., Zaki, W.N., 1954. Sedimentation and fluidisation: part I. Trans. Inst. Chem. Eng. 32, 35–53.

Schoumans, O.F., Bouraoui, F., Kabbe, C., Oenema, O., van Dijk, K.C., 2015. Phosphorus management in Europe in a changing world. Ambio 44 (2), S180–S192.

Sterling, M.S., Ashley, K.I., 2003. Evaluations of slow-release fertilizer for rehabilitating oligotrophic streams. Am. Fish. Soc. Symp. 34, 237–243.

Syamlal, M., O'Brien, T.J., 1989. Computer simulation of bubbles in a fluidized bed. AIChE Symp. Ser. 85, 22–31.

Vedantam, S., Ranade, V.V., 2013. Crystallization: key thermodynamic, kinetic and hydrodynamic aspects. Sadhana 38 (38), 1287–1337.

Wang, S., Li, X., Wu, Y., Li, X., Dong, Q., Yao, C., 2010. Simulation of flow behavior of particles in a liquid–solid fluidized bed. Ind. Eng. Chem. Res. 49, 10116–10124.

Wen, C.Y., Yu, Y.H., 1966. Mechanics of fluidization. Chem. Eng. Prog. Symp. Ser. 62, 100–111.

Xia, Q., Chen, C., 2007. Unit Operations of Chemical Engineering. Tianjin University Press, Tianjin, pp. 40–43.

Yan, W.C., Luo, Z.H., Guo, A.Y., 2011. Coupling of CFD with PBM for a pilot-plant tubular loop polymerization reactor. Chem. Eng. Sci. 66, 5148–5163.

Ye, Z.L., Shen, Y., Ye, X., Zhang, Z., Chen, S., Shi, J., 2014. Phosphorus recovery from wastewater by struvite crystallization: property of aggregates. J. Environ. Sci. 26 (5), 991–1000.

Ye, X., Ye, Z.L., Lou, Y., Pan, S., Wang, X., Wang, M.K., et al., 2016. A comprehensive understanding of saturation index and upflow velocity in a pilot-scale fluidized bed reactor for struvite recovery from swine wastewater. Powder Technol. 295, 16–26.

Zheng, Y., Zhu, J., 2003. Radial distribution of liquid velocity in a liquid–solids circulating fluidized bed. Int. J. Chem. React. Eng. 1 (1), 1–7.